Measurement of third-order nonlinear optical susceptibility of synthetic diamonds

Jianxun Zhao (赵建勋)[1], Gang Jia (贾 刚)[1], Xiuhuan Liu (刘秀环)[2], Zhanguo Chen (陈占国)[1*], Jie Tang (唐 杰)[3], and Shuang Wang (王 爽)[1]

[1]*State Key Laboratory on Integrated Optoelectronics, College of Electronic Science and Engineering, Jilin University, Changchun 130012, China*

[2]*College of Communication Engineering, Jilin University, Changchun 130012, China*

[3]*Applied Technique College, Jilin University, Changchun 130012, China*

[*]*E-mail: czg@jlu.edu.cn*

Received March 3, 2010

Diamonds are wide-gap semiconductors possessing excellent physical and chemical properties; thus, they are regarded as very appropriate materials for optoelectronic devices. Based on the Kerr effect, we introduce a simple and feasible method for measuring the third-order nonlinear optical susceptibility of synthetic diamonds. In the experiments, synthetic type I diamond samples and transverse electro-optic modulation systems are utilized. As for the laser with the wavelength of 650 nm, the third-order susceptibility and Kerr coefficient of the diamond samples are obtained at $\chi^{(3)}_{1212} = 2.17 \times 10^{-23}$ m^2/V^2 and $S_{44} = 1.93 \times 10^{-23}$ m^2/V^2, respectively.

OCIS codes: 160.4670, 190.3270, 160.4760.

doi: 10.3788/COL20100807.0685.

Diamonds have been studied as wide-gap semiconductors with a bandgap of about 5.5 eV[1]. They have been found to possess excellent optical and electronic properties, such as high breakdown field ($\sim 10^7$ V/cm), high carrier mobility ($\sim$0.2 m^2/(V·s))[2], high thermal conductivity ($\sim$20 W/(cm·K))[3], high resistivity ($\sim 10^{16}\,\Omega$·cm), low dielectric constant (5.66)[4], and good transparency over a wide range of electromagnetic spectra from 225 nm to the far infrared[5]. For these reasons, diamonds have been regarded as very suitable materials for optoelectronic devices. The technology improvement on, and the price decrease of large-sized synthetic diamonds have promoted the application and further development of diamonds. For example, artificial diamond sensors have been widely used for detecting radiation[6], charged particles[7], temperature[8], etc. Diamonds belong to the m3m point group and have inverse symmetry. According to the dipole approximation, the second-order nonlinear optical effects should be forbidden. The third-order nonlinear optical effects have been considered as the main nonlinear phenomena in diamonds. In order to utilize these third-order nonlinear optical effects, the third-order nonlinear susceptibility of diamonds must be determined. However, only a few related reports have been published. Anastassakis *et al.* observed the second-order electro-optic effect (Kerr effect) in natural type IIa diamonds[9]. They used a well-known method based on the elliptical properties of the light emerging from a birefringent crystal placed between two crossed polarizers and measured the total phase difference to estimate the Kerr coefficient. However, the error of this method was considerable, and only the order of magnitude of the Kerr coefficient was estimated at a wavelength of 546.1 nm. Arya *et al.* calculated the third-order nonlinear optical susceptibility tensor in diamond by the tight-binding orbital model[10]. Levenson *et al.* investigated the details of the dispersive behavior of the third-order nonlinear optical susceptibility tensor in natural and synthetic diamonds by frequency mixing experiments[11]. The set of experimental equipment used in their investigations was complex and expensive.

In this letter, a nonzero element of the third-order nonlinear optical susceptibility tensor $\chi^{(3)}_{1212}$ of synthetic type I diamonds is investigated at a wavelength of 650 nm using the transverse electro-optical (EO) modulation system and the theory of Kerr effect. This method requires affordable experimental equipment and very simple experimental processes, while providing high measurement precision at the same time.

Diamonds belong to cubic crystal class, and their refractive indices have been found to be isotropic. Without the external fields, the index ellipsoid of diamonds would be a sphere. If an external electric field is applied on the diamond crystal, symmetry will be reduced and it will become a birefringent crystal. The change of refractive index has been found to be proportional to the square of the intensity of the applied electric field. When the applied electric field is along the direction of [111] of the diamond crystal, it has been found that the diamond crystal could change into a uniaxial crystal whose optical axis is the [111] crystallographic axis. The index ellipsoid will then become a rotational ellipsoid whose axis of rotation is also the [111] crystallographic axis.

The ideal shape of diamond crystal is cuboctahedron, as shown in Fig. 1(a). The samples used in our experiments were provided by Zhengzhou Zhongnan Jete Superabrasives Co., Ltd. As shown in Fig. 1(b), these samples are irregular cuboctahedrons and include eight hexagonal planes and six quadrilateral planes. All the hexagonal faces are {111} planes, and the quadrilateral faces are {100} planes. The two opposite hexagonal planes or opposite quadrilateral planes are parallel to

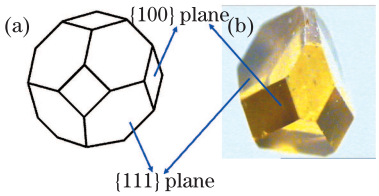

Fig. 1. Illustration of the diamond sample used in the experiment. (a) Ideal shape of the diamond crystal–cuboctahedron; (b) photograph of the diamond sample.

each other. Pure diamond crystals are transparent and colorless. In our experiments however, unintentionally doped type I diamond crystals were used. These crystals are yellowish because of the presence of trace quantities of nitrogen impurities in the crystals. Despite of the impurities, the resistivity of the diamond samples is still high (about $10^8\,\Omega\cdot$cm), and the carrier density is only about $3\times10^7\,\mathrm{cm}^{-3}$ at room temperature. Thus, the carrier effect can be ignored.

When the modulating electric field $\boldsymbol{E}=\boldsymbol{E_0}\cos(\omega t)$ is applied on the diamond sample along the [111] axis ($\boldsymbol{E}$ is the applied electric field), according to the theory of Kerr effect[12], the refractive index along the optical axis ([111] axis, which is also selected as the z axis in the Cartesian coordinates) can be written as

$$n_z = n_0 - n_0^3 E_0^2 (S_{11}+2S_{12}+2S_{44})/6, \tag{1}$$

where S_{ij} is the Kerr coefficient, n_0 is the refractive index of the diamond without electric field application, and E_0 is the intensity of the applied electric field. According to the relationship between the Kerr coefficient S_{ijkl} and the third-order susceptibility element, $S_{ijkl}=-3\chi^{(3)}_{ijkl}/\varepsilon^0_{ii}\varepsilon^0_{jj}$, Eq. (1) can be rewritten as

$$n_z = n_0 + E_0^2\left(\chi^{(3)}_{1111}+2\chi^{(3)}_{1122}+2\chi^{(3)}_{1212}\right)/2n_0, \tag{2}$$

where $\chi^{(3)}_{1111}$, $\chi^{(3)}_{1122}$, and $\chi^{(3)}_{1212}$ are the nonzero elements of the third-order nonlinear optical susceptibility of diamond. Similarly, the refractive indices along the directions perpendicular to the [111] axis (e.g., the $[1\bar{1}0]$ and $[11\bar{2}]$ axes corresponding to the x and y axes in the Cartesian coordinates, respectively) can be expressed as

$$n_x = n_y = n_0 + E_0^2\left(\chi^{(3)}_{1111}+2\chi^{(3)}_{1122}-\chi^{(3)}_{1212}\right)/2n_0. \tag{3}$$

Thus, when the probing beam is perpendicular to the direction of the applied electric field, the maximum phase delay $\Delta\phi_{\max}$ can be obtained. That is,

$$\Delta\phi_{\max} = 3\pi L E_0^2 \chi^{(3)}_{1212}/\lambda n_0, \tag{4}$$

where L is the optical path in the diamond sample under the electric field, and λ is the wavelength of the probing beam in vacuum. However, because diamond is the hardest material, abrasion and processing into the required shape are difficult. Thus, based on the original geometry shape of the diamond samples, the $[11\bar{1}]$ axis was chosen as the propagation direction of the probing beam, which was tilted at an angle of $\theta=70.53°$ with respect to the optical axis. The two normal modes of the probing beam in $(11\bar{1})$ plane, namely, the o-ray and e-ray, will experience the respective refractive indices as

$$n_{\mathrm{o}} = n_0 + E_0^2\left(\chi^{(3)}_{1111}+2\chi^{(3)}_{1122}-\chi^{(3)}_{1212}\right)/2n_0, \tag{5}$$

$$n_{\mathrm{e}} = n_0 + E_0^2\left(\chi^{(3)}_{1111}+2\chi^{(3)}_{1122}+5\chi^{(3)}_{1212}/3\right)/2n_0. \tag{6}$$

As a result, the phase difference between the o-ray and e-ray can be written as

$$\Delta\phi = 8\pi L E_0^2 \chi^{(3)}_{1212}/3\lambda n_0. \tag{7}$$

The sample was bounded by two steel electrodes. In order to avoid the air gap between the electrode and the sample, soft indium slices were sandwiched between the electrode and the sample. The electrodes were then surrounded by insulating glue to prevent discharging, and tightly contacted with the opposite (111) planes. Each contact area was slightly smaller than the face of the sample. The sample and the electrodes were fixed on an insulating board with a hole at the center, so that the probing beam can travel through the sample and the hole. The configuration of the electrodes is shown in Fig. 2. In the experiments, it was necessary to apply very high alternating current (AC) voltage on the sample. The output signal from the low-frequency signal generator was coupled into an audio power amplifier to obtain a higher power signal, and then this high power signal was transformed into the required AC voltage by a transformer.

A transverse EO modulation system was set up, as shown in Fig. 3. A 650-nm continuous-wave (CW) laser diode was used as the light source, and the probing beam was received by the Si photodetector connected with the lock-in amplifier. The $[11\bar{1}]$ axis was horizontal in the space. The vertical orientation in the space was named y' axis. The polarization of the polarizer was 45° with respect to the y' axis, and the polarization of the analyzer was perpendicular to that of the polarizer. The fast axis of the quarter wave plate was parallel to the y' axis. Lens 1 focused the beam into the sample, and the output beam from the sample was collimated by lens 2 whose focal distance was the same as lens 1. Both lenses were long-focus lens, so that the beam in the sample can still be taken as the parallel beam. Under these conditions, the system will meet the best sensitivity and linearity, and the intensity of the output beam from the analyzer can be calculated using the Jones matrix[13]:

$$I_{\mathrm{out}} = I_{\mathrm{in}}(1+\sin\Delta\phi)/2, \tag{8}$$

where I_{in} is the intensity of the input beam, and $\Delta\phi$ is the phase difference expressed in Eq. (7). Generally, $\Delta\phi \ll 1$, thus Eq. (8) can be rewritten as

$$I_{\mathrm{out}} = I_{\mathrm{in}}\left(1+8\pi E_0^2 L\chi^{(3)}_{1212}/3\lambda n_0\right)/2. \tag{9}$$

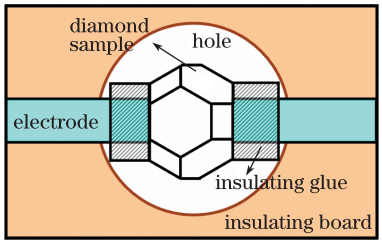

Fig. 2. Top view of the electrode configuration.

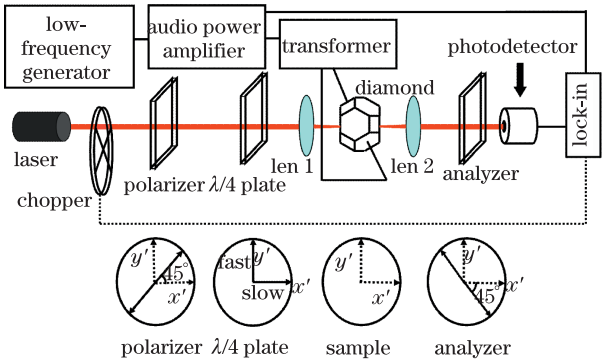

Fig. 3. Experimental setup for the transverse EO modulation system.

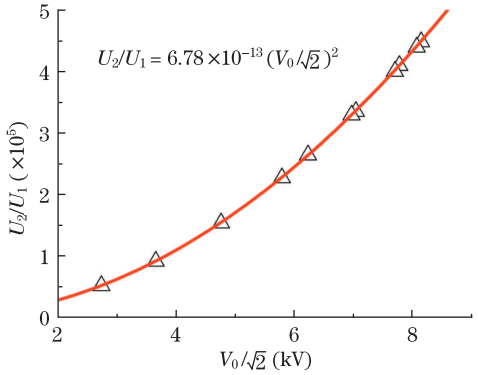

Fig. 4. Relationship between U_2/U_1 and $V_0/\sqrt{2}$.

Assuming that the modulation voltage $V = V_0 \cos \omega t$ is applied on the sample, and d is the distance between the electrodes, the electric field could be expressed as $E_0 = V/d = V_0(\cos \omega t)/d$, and Eq. (9) could be changed into

$$\begin{aligned} I_{\text{out}} &= I_{\text{in}} \left(1 + 4\pi V_0^2 L \chi^{(3)}_{1212}/3\lambda n_0 d^2\right)/2 + \tilde{I}(2\omega) \\ \tilde{I}(2\omega) &= 2\pi I_{\text{in}} V_0^2 L \chi^{(3)}_{1212} \cos(2\omega t)/3\lambda n_0 d^2 \end{aligned}. \quad (10)$$

From Eq. (10), the output beam includes the direct current (DC) component which cannot be detected by the lock-in amplifier, and the AC component $\tilde{I}(2\omega)$ which can be detected.

Without modulation voltage on the sample, the intensity of the output beam from the analyzer, that is, $I_1 = I_{\text{in}}/2$, can be detected by the Si photodetector and the lock-in amplifier after chopping the probing beam at the frequency of 284 Hz. The measured photoelectric signal is $U_1 = MI_1 = MI_{\text{in}}/2 = 45.9$ mV, where M is a factor relevant to the optical elements and the responsivities of the photodetector and the lock-in amplifier. The chopped optical signal received by the photodetector is the square wave, which can be expressed in the form of the Fourier series; however, the lock-in amplifier can only detect the sine signal at the fundamental frequency, thus a modification factor $2/\pi$ is considered as[14]

$$U_1 = 2MI_1/\pi = MI_{\text{in}}/\pi = 45.9 \text{ mV}. \quad (11)$$

Then, with the chopper removed, the modulation voltage with the frequency of 142 Hz was applied on the sample. The frequency of the reference channel of the lock-in amplifier was set at twice the frequency of the modulation voltage. Thus, the AC component $\tilde{I}(2\omega)$ can be detected, and the measured photoelectric signal U_2 can be written as

$$U_2 = M\left|\tilde{I}(2\omega)\right| = 2\pi M I_{\text{in}} L V_0^2 \chi^{(3)}_{1212}/3\lambda n_0 d^2. \quad (12)$$

From Eqs. (11) and (12), we obtain the ratio of U_2 and U_1 as

$$U_2/U_1 = 2\pi^2 L V_0^2 \chi^{(3)}_{1212}/3\lambda n_0 d^2. \quad (13)$$

The relationship between U_2/U_1 and $V_0/\sqrt{2}$ can be measured by altering the amplitude of the modulation voltage, as shown in Fig. 4. A good quadratic curve was derived using this process. From the fitting function, we obtained the coefficient of the quadratic term as

$$2\pi^2 L \chi^{(3)}_{1212}/3\lambda n_0 d^2 = 3.39 \times 10^{-13} \text{ V}^{-2}. \quad (14)$$

The distance between the electrodes and the optical path were measured by a vernier caliper, and the values were obtained at $d = 1.95$ mm and $L = 1.41$ mm, respectively. The refractive index of the diamond was $n_0 = 2.4105$ at the wavelength of 650 nm. Thus, from Eq. (14), the third-order nonlinear optical susceptibility element $\chi^{(3)}_{1212} = 2.17 \times 10^{-22}$ m^2/V^2 was obtained. According to the relationship between the Kerr coefficient and the third-order susceptibility element, the Kerr coefficient of diamonds can also be achieved, that is, $S_{44} = S_{1212} = 1.93 \times 10^{-23}$ m^2/V^2.

Measuring the absolute intensity of the probing beam thus became unnecessary, and later became an advantage. Moreover, the transverse EO modulation system was designed to meet the best sensitivity and linearity; the phase delay whose measurement should be as large as possible was realized according to the original shape of diamond samples. All these ensured measurement precision.

However, the intensity fluctuations of the laser resulted in 2% error because the values of U_1 and U_2 were not measured synchronously. Given that the propagation direction of the probing beam is not perpendicular to the optical axis of the diamond in experiments, there exists a walk-off angle α between the o-ray and e-ray. α can be estimated according to[15]

$$\tan\alpha = \left(1 - n_y^2/n_z^2\right) \frac{\tan\theta}{1 + n_y^2 \tan^2\theta/n_z^2}. \quad (15)$$

Given the insignificant difference between n_y and n_z, the walk-off angle α in our experiments was very small, a negligible value of about 10^{-6}. The wavelength of the laser was 650 nm, a value far from the absorption edge of diamond (~225 nm); thus, the Franz-Keldysh effect was omitted[16]. In addition, since the carrier density in the diamond samples was very low, the carrier effects, such as free-carrier dispersion effect[17], electric field shield effect of carriers, etc., were ignored as well.

In conclusion, we present a general method for measuring the third-order nonlinear optical susceptibility of wide bandgap materials. The method is very convenient and feasible because measuring the absolute intensity of the probing beam is rendered unnecessary. One of

the obtained third-order nonlinear optical susceptibility elements $\chi^{(3)}_{1212}$ of diamond crystals has the same order of magnitude as that in a previous study[11]. The possibility of achieving other third-order susceptibilities $\chi^{(3)}_{1111}$ and $\chi^{(3)}_{1122}$ using this method is presented particularly when the suitable crystal orientations and the directions of applied electric fields are adopted. Consequently, the Kleinman symmetry of diamonds can be verified. With the breakdown field of diamonds of about 10^7 V/cm, the diamond crystal with 1-mm thickness can endure a breakdown voltage of 10^6 V. Diamonds have potential applications in high voltage sensors based on the Kerr effect.

This work was supported by the National Natural Science Foundation of China (Nos. 60976043 and 60976037), the Collaborative Projects of NSFC-RFBR Agreement (Nos. 60711120182 and 60811120023), and the National "863" Program of China (No. 2009AA03Z419).

References

1. S. Almaviva, M. Marinelli, E. Milani, G. Prestopino, A. Tucciarone, C. Verona, G. Verona-Rinati, M. Angelone, and M. Pillon, Diamond Relat. Mater. **18,** 101 (2009).
2. Z.-C. Dong, A. S. Trifonov, N. V. Suetin, and P. V. Minakov, Surface Science **549,** 203 (2004).
3. S. M. Baker, G. R. Rossman, and J. D. Baldeschwieler, J. Appl. Phys. **74,** 4015 (1993).
4. M. I. Eremets, Semicond. Sci. Technol. **6,** 439 (1991).
5. P. Olivero, S. Rubanov, P. Reichart, B. C. Gibson, S. T. Huntingtor, J. Rabeau, A. D. Greentree, J. Salzman, D. Moore, D. N. Jamieson, and S. Prawer, Advanced Materials **17,** 2427 (2005).
6. Y. Koide, M.Y. Liao, and M. Imura, Diamond Relat. Mater. **19,** 205 (2010).
7. E. Berdermann, K. Blasche, P. Moritz, H. Stelzer, and B. Voss, Diamond Relat. Mater. **10,** 1770 (2001).
8. Y. Koide, M. Y. Liao, J. Alvarez, M. Imura, K. Sueishi, and F. Yoshifusa, Nano-Micro Lett. **1,** 30 (2009).
9. E. Anastassakis and E. Burstein, J. Opt. Soc. Am. **61,** 1618 (1971).
10. K. Arya and S. S. Jha, Phys. Rev. B **20,** 1611 (1979).
11. M. D. Levenson and N. Bloembergen, Phys. Rev. B **10,** 4447 (1974).
12. A. Yariv and P. Yeh, (eds.) *Optical Waves in Crystals: Propagation and Control of Laser Radiation* (John Wiley & Sons Inc., New York, 1984).
13. Z. Chen, J. Zhao, Y. Zhang, G. Jia, X. Liu, C. Ren, W. Wu, J. Sun, K. Cao, S. Wang, and B. Shi, Acta Opt. Sin. (in Chinese) **29,** 1336 (2009).
14. K. Cao, Z. Chen, C. Ren, G. Jia, T. Zhang, X. Liu, B. Shi, and J. Zhao, Microelectronics J. **40,** 70 (2009)
15. J. Li, B. Zhu, and G. Wei, (eds.) *Crystal Optics* (in Chinese) (Beijing Institute of Technology Press, Beijing, 1989) p.83.
16. Y. Zhang, Z. Chen, G. Jia, B. Shi, C. Ren. X. Liu, and W. Wu, J. Infrared Millim. Waves (in Chinese) **27,** 165 (2008).
17. R. A. Soref and B. R. Bennett, IEEE J. Quantum Electron. **23,** 123 (1987).